Effect of Surface Roughness on Steel-Steel Dry Friction Coefficient

H. Charsetad[1], S.M. Khorsandijou[2*]

Abstract: The influence of surface roughness magnitude and direction on dry static friction coefficient between two similar steel samples has been studied through an experiment. A testing apparatus has been designed and fabricated to measure the friction coefficient for a few forms of surface asperity. The average, maximum and minimum values of static friction coefficients among steel samples have been measured and numerically proposed in terms of some discrete values of the surface roughness, base and counter body angles. Correction coefficient defined as the ratio of maximum to minimum friction coefficient has been found on the result basis. According to the results of the experiments, dry static friction coefficient between two similar steel samples is affected by both magnitude and direction of surface roughness. Under the condition of static equilibrium, the Colomb - Amonton formula has been used to determine friction coefficient between samples. The flexibility and mass of the string have been neglected, and the reservoir pendulum-like swinging and the water movement therein have been avoided within the experiments.

1. Introduction

External friction of solids is a complex phenomenon depending on different processes that occur in the real areas of contact and in thin surface layer during relative tangential movement of the bodies. The coefficient of friction is the ratio of the sliding friction force to the normal component of the external forces that act on the rubbing surfaces [1]. Friction coefficient between two sliding bodies depends on composition of mating materials, velocity of relative motion, nature of the contact, temperature of interfacial areas, history of previously sliding surfaces, the force holding the solids in contact, nature of relative motion, surface finishing status, characteristics of the machine and fixtures within which the materials are clamped and the ambient factors such as humidity and pressure [2].

Using a pin-on-plate sliding tester, the effect of surface texture on friction coefficient and transfer-layer formation during sliding has been studied [3]. Wearing particle debris density and friction coefficients have been studied for a few different hardness values of steel specimens in dry sliding pin-on-disc tests [4]. Shot pining processes has a long-term increase on friction [5]. Surface preparation deals with roughness

1. Ms. C., South Tehran Branch, Islamic Azad University, Tehran, Iran (charsetad.hossein@gmail.com)
2*. Corresponding Author: Assistant Professor, South Tehran Branch, Islamic Azad University, Tehran, Iran (m_khorsandijou@azad.ac.ir)

parameters that influence the friction coefficient [6]. Macro-particles severely alter the geometric surface parameters and eventually the friction coefficient [7]. The dry sliding friction depends upon surface roughness and temperature at atomic scale [8]. By pin-on-disc testing on steel surface, the relationship between standard surface roughness parameters and friction has been found. The surfaces with negative S_{sk} and higher S_{ku} have lower friction [9].

The effect of surface texture and roughness parameters on aluminum pin slipping on a grinded steel sheet has been studied. It has been found that plowing and adhesion are independent from surface roughness and are controlled by surface texture [10]. By considering the components of friction in elasto-plastic defor-mation, it was revealed that the increase in elastic modulus increases the effective friction coefficient between the spherical asperities [11]. Summit height and radius of asperities in rough surfaces of an isotropic material have been studied, and a detailed description about the dimensional parameters has been exposed [12].

Based on the twist and compression, a testing machine has been designed and used to determine the friction coefficient between aluminum and steel in elastic-plastic zone. It has been found that friction coefficient between aluminum and steel starts from 0.2 and increases up to 0.8 in elastic region and finally decreases down to 0.6 in plastic region [13]. During metal forming operation, surface texture has been taken into consideration. It has been found that during stick-slip motion, the friction coefficient in transfer-layer formation depends on the surface texture and roughness of the tools [14]. In reciprocating motion, dry and lubricated friction coefficient and transfer-

layer formation depend upon the surface texture of the plate [15].

For plates being unidirectional, grounded and randomly-directional surface textures, friction coefficient and transfer-layer formation depend on surface texture during the first five cycles [16]. Friction coefficient depends on the average slope of the surface asperities [17]. The effect of surface texture of steel sheet in contact with a polymer pin has been studied. The friction coefficient and transfer-layer formation are related to the components of plowing and adhesion [18]. Using finite element methods, the friction and plastic deformation have been examined in macro scale [19]. Interaction effects of asperity contact behavior of elastically roughed surfaces have been analytically studied. The analytical results have been compared with that of Greenwood-Williams-based models and other experimental measurements [20]. Micro cases of asperity contact used in asperity lines deformation have been studied [21].

The finite element software of Abaqus has been used to study the effects of spherical and cylindrical asperities on the friction conditions of a sliding elasto-plastic deformation. Analytical results are used to predict the friction coefficient of surfaces with random asperities [22]. The friction coefficient of steal-aluminum contact surfaces has been determined in a few 0.75-second intervals [23]. By the Consideration of the effect of surface texture tools on friction coefficient, reveals that the slipping friction coefficient and transfer layer formation depend on the grinding direction [24]. In the field of surface roughness and contact-surface topography, the relationship between friction and surfaces roughness could be observed [25].

The present paper deals with an experiment showing the influence of magnitude and direction of the surface asperity on the static dry friction coefficient between two similar steel samples with approximately similar asperities. Similar asperity grooves have been created on the samples. The rough surfaces of the samples are put in contact with a gravitationally-created pressure, while the asperity groove directions are making an adjustable desired angle. A testing apparatus has been designed and fabricated for the measurement of static friction coefficient with respect to different adjustable angles of the base and counter bodies.

2. Experiment Setup

2.1. Sample preparation

Six steel cylindrical samples have been manufactured by a lathe machine for the experiment of the present article. Samples shown by Fig. 1 are 50 mm in diameter and 30 mm in height. Surface of the samples has been polished by a grinding machine. The experiment has been established on the basis of parallel grooves of asperity on the flat surfaces of the samples. So, in order to generate the grooves, one flat surface of the samples has been rubbed over an abrasive paper with a definite grade of asperity. Before using abrasive paper the average surface hardness number of the samples has been measured 223 V (DPH) by the hardness measuring instrument of MACRO under the ambient temperature of 24°C and relative humidity of 29 %. The steel samples have to be cleaned before each test with ethanol and a nap-free fabric.

For each sample the rubbing direction has been tried to be preserved constant. Constant by it is essential for the parallel grooves to be constructed properly. Otherwise a previously created groove would be destroyed by the next rubbing action. In this article, using three grades of abrasive papers, i.e. P100, P220 and P400, three sample categories have been generated. For the samples of each category the pressure and repetition of the rubbing action have been tried to be held unchanged. The grades of the abrasive papers used for the preparation of the lower and upper samples of each test have been held exactly the same. The surface roughness of rubbing surfaces caused by applying the abrasive paper is calculated by the use of Table 1 and interpolation [26]. Average surface roughness due to the abrasive papers with the grades of P100, P220 and P400 is expected to be 1.1, 0.3 and 0.2 respectively.

The testing device shown by Fig. 2 has been used for the measurement of static friction coefficient between steel samples.
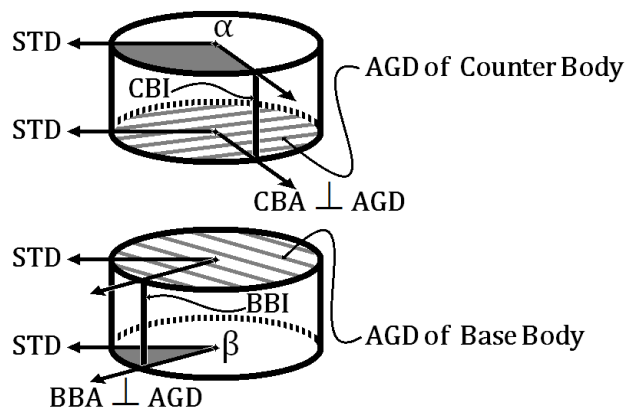

Fig. 1. Upper and lower steel samples.

There is an index over the stand of this apparatus. The stand index is a guide determining the string or the pulling load direction. In the present article slide tendency direction, i.e. STD, has been assumed to be coincided with the pulling load direction. As shown by Fig. 1, the upper and lower steel samples are called counter and base bodies respectively. Each counter or base body has been provided with an index, namely CBI and BBI. These indexes are guides for the body axes of the upper and lower samples. These axes, i.e. CBA and BBA, are the radial directions perpendicular to the asperity groove directions, i.e. AGD, of the samples.The angular distance of counter and base body indexes with respect to the stand index are respectively called the counter and base body angles. The directions of the counter and the base bodies with respect to STD are respectively symbolized by the angles α and β being depicted by Fig. 1.
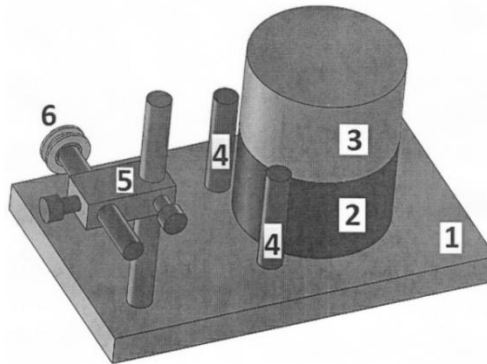
Each sample has been provided with a lateral label showing its mass and average surface roughness. The number zero on the lateral label of the counter and base bodies are corresponding to the body indexes CBI and BBI.

Sample preparation by rubbing over abrasive paper in major, and sample sliding in each experiment in minor erodes the samples. As a consequence, the base and counter bodies lose some little part of their masses. Due to this reason before each individual experiment the mass of the samples has been measured by a digital scale having the accuracy of 0.01 g. The weight of counter body generates the contact pressure required for friction between the two samples. In the first three experiments the masses of the components have been measured and shown by Table 2.

Table 1. Average surface roughness on steel caused by the grade of abrasive paper [26]

Standard ANSI grit	European P-grade	Median diameter (µm)	Surface roughness on steel, R_a (µm)
60	P60	250	
80	P80	180	1.140
120	P120	106	1.050
180	P180	75	0.880
240	P220	63	0.300
320	P360	40.5	0.230
400	P800	25.8	0.120
600	P1200	15.3	0.110
800	P2400	6.5	0.025
1200	P4000	2.5	0.020

Fig. 2. Apparatus for the measurement of the friction coefficient.

2.2. Testing apparatus

Considering Fig. 1, the counter body is located on the base body. The apparatus illustrated by Fig. 2 has been designed to let the counter body arrive at the threshold of movement. The counter body gets to the situation of slide threshold on the base body due to a particular magnitude of the string tension or the pulling load. The data of the experiments have been recorded under the mentioned situation. Using this device, static friction coefficient between two steel samples has been measured in various directions of the pulling load with respect to the AGD of the lower and upper steel samples. The apparatus restricts the counter body to move along the STD.

The formulation of this article has neglected the vertical and lateral motions thereof. The apparatus is designed so that the load magnitude would be linearly increased versus time. Construction cost of this apparatus is low however the parallelism and flatness of the surfaces have been achieved. The results of this article show that the measurement accuracy thereof is appropriate. Fundamental components of the apparatus shown by Fig. 2 are: (1) Stand on top of which the base body is located. (2) Base body which is the lower steel sample. (3) Counter body which is the upper steel sample and is fixed by a Clamp. (4) Stoppers which limit the motion and prevent the sample from dropping. (5) Position regulator and (6) Spool which is the pulley-shaped object around which the thread or string is wound.

2.3. Testing instructions

Pressure, temperature and relative humidity of the testing room of the present article have been recorded 1 atmosphere, $25\pm2°C$ and $40\pm10\%$ respectively. The steel samples have been cleaned by ethanol and a nap-free fabric before each test. According to Fig. 1, the two samples are vertically located over each other. It is essential that the asperities of their flat surfaces are in contact. Considering BBI, CBI and the index existing on the stand of the apparatus shown by Fig. 2, one can respectively fix the base and counter bodies at the angels of β and α with respect to STD. The clamp is then firmly installed over the counter body to keep the magnitude of α. Stoppers are then installed in their specified locations. When the clamp is unfastened, the angle of counter body, i.e. α can be freely adjusted at a desired value. Then by fastening the clamp the counter body is fixed.

At this stage the samples are ready to be tested. Four AGD arrangements have been shown by Fig. 3.

Water starts to be slowly poured into the reservoir with the volume flow rate of 17 millilitre per minute. This constant volume flow rate linearly increases the magnitude of the string tension, i.e. T. At a particular moment the total weight of reservoir and the water therein reaches a particular magnitude required for the pulling load to drag the counter body with a constant velocity relative to the base body. This situation is a little bit after the sliding threshold, so the resultant friction force is nearly equal to the total weights of the reservoir and water.

3. Static equilibrium

Free body diagrams of counter body and the whole system of counter and base bodies before the slide of counter body over base body have been illustrated by Figs. 4(a & b). It should be noted that only the resultant of the distributed contact loads, i.e. F, N and n have been depicted in these figures. Friction force, i.e. F is proportional to the contact normal force, i.e. N.

Table 2. Masses of the components in the first three experiments.

Number of experiment	Mass of base body M_b (g)	Mass of counter body M_c (g)	Mass of clamp M_d (g)	Mass of reservoir M_r (g)
1	447.40	450.10	21.04	19.14
2	446.60	450.00	21.04	19.14
3	446.70	449.90	21.04	19.14

(a) Counter body angle α=0° and base body angle β=0°

(b) Counter body angle α=0° and base body angle β=90°

(c) Counter body angle α=90° and base body angle β=90°

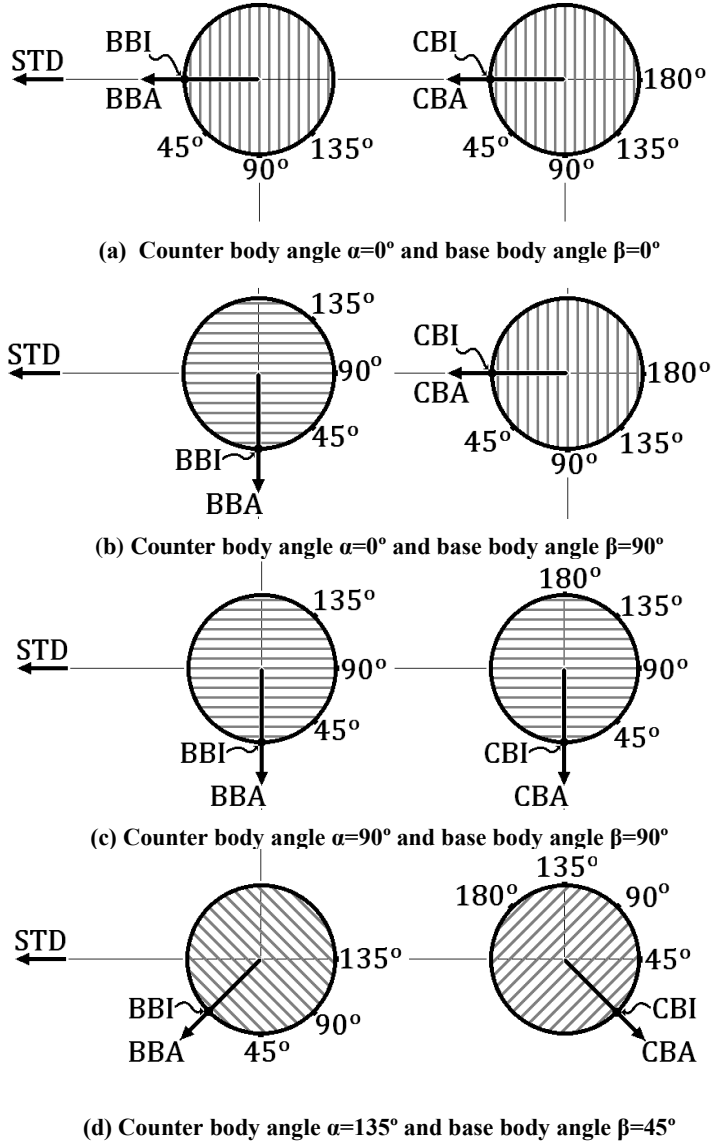(d) Counter body angle α=135° and base body angle β=45°

Fig. 3. Four AGD arrangements for the upper and lower steel samples.

$$F = f\ N \tag{1}$$

Eq. (1) indicates that the friction coefficient symbolized by f is the ratio of friction over normal force. Based on the static equilibrium condition, the force balance of counter body along vertical and STD directions are respectively given by Eqs. (2) and (3).

$$N = M_c\ g + M_{Ci} g \tag{2}$$

$$F = T \tag{3}$$

The string mass and flexibility, the pendulum-like swinging of string-reservoir system, reservoir and string acceleration and the movement of the water within the reservoir have all been assumed negligible. Therefore, one can easily find the magnitude of the string tension with the aid of Eq. (4).

$$T = M_W g + M_R g \tag{4}$$

By substitution of T from Eq. (4) into Eq. (3) and then by substitution of N and F from Eqs. (2) and (3) into Eq. (1) one can obtain the Colomb-Amonton formula, i.e. Eq. (5). It gives the static friction coefficient between upper and lower samples. The experimental results of this article confirm the validity of this equation.

$$f = \frac{M_W + M_R}{M_C + M_{Ci}} \tag{5}$$

4. Results and discussion

Static friction coefficient between two steel samples versus counter body angle has been experimentally determined for four values of the base angle, i.e. 0°, 45°, 90° and 135°. Three values of average surface roughness, i.e. 0.2, 0.3 and 1.1 micron, have been considered for the samples of the experiments. The results have been respectively depicted by Figs. 5 (a, b & c). They show that surface asperity effectively influences the friction coefficient.
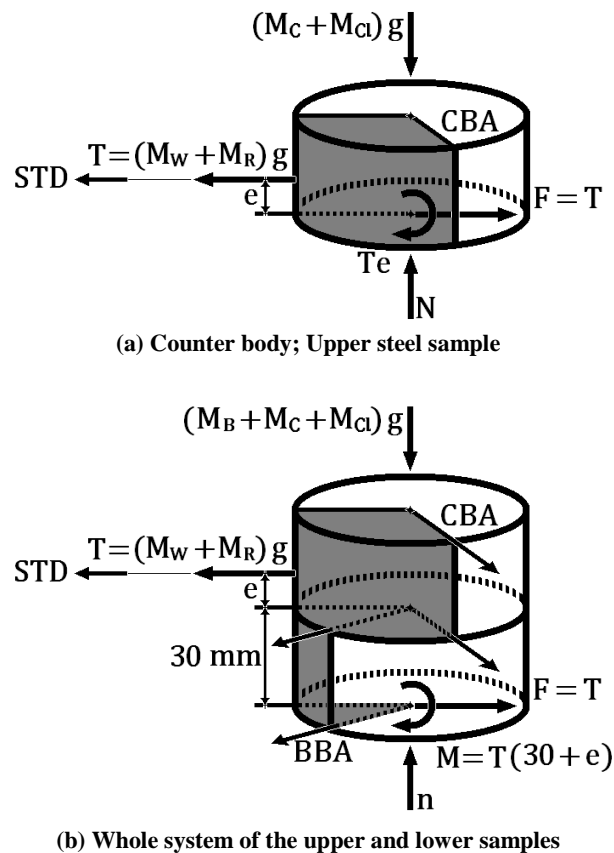

(a) Counter body; Upper steel sample

(b) Whole system of the upper and lower samples

Fig. 4. Free body diagram before the relative motion of the samples.

Four magnitudes, i.e. 0º, 45º, 90º and 135º and five magnitudes, i.e. 0º, 45º, 90º, 135º and 180º have respectively been considered for the base and counter body angles, i.e. β and α. Eventually the data of twenty experiments have been recorded by the present article. These experiments have been repeated five times, but only their averages have been recorded. Four arrangements out of the mentioned twenty AGD arrangements have been shown by Fig. 3. The result of each experiment depends upon the average surface roughness, i.e. R_a and the angles α and β.

Considering Fig. 5(a), static friction coefficient between two cylindrical steel samples having sizes equal to those of this article and having average surface roughness of 0.2 μm, has minimum and maximum values respectively at α=90º and α=0º,when β is 0º or 45º. It has minimum and maximum values respectively at α=0º and α=180º when β is 90º. It has minimum and maximum values respectively at α=45º and α=180º when β is 135º. Comparing the results of the twenty experiments recorded on the diagram of Fig. 5(a), the maximum value of the static friction coefficients, i.e. 0.340332, occurs under the situation of β=90º and α=180º, and its minimum value, i.e. 0.163331, occurs under the situation of β=0º and α=90º. Maximum difference between the obtained static friction coefficients of Fig. 5(a) is equal to 0.177001. The correction coefficient that is defined as the ratio of maximum to minimum static friction coefficient is equal to 2.083695.

Considering Fig. 5(b), static friction coefficient between two cylindrical steel samples having sizes equal to those of this article and having average surface roughness of 0.3 μm, has minimum and maximum values respectively at α=135º and α=90º,when β is 0º or 135º. It has minimum and maximum values

respectively at α=90º and α=180º when β is 45º. It has minimum and maximum values respectively at α=45º and α=0º when β is 90º. Comparing the results of the twenty experiments saved on the diagram of Fig. 5(b), the maximum value of the static friction coefficients, i.e. 0.372557, occurs under the situation of β=45º and α=180º, and its minimum value, i.e. 0.147429, occurs under the situation of β=0º and α=135º. Maximum difference between the obtained static friction coefficients of Fig. 5(b) is equal to 0.225128. The correction coefficient that is defined as the ratio of maximum to minimum static friction coefficient is equal to 2.527027.

Considering Fig. 5(c), static friction coefficient between two cylindrical steel samples having sizes equal to that of this article and having average surface roughness of 1.1 μm, has a minimum and maximum value respectively at α=90º and α=135º,when β is 0º. It has a minimum and maximum value respectively at α=0º and α=180º when β is 45º. It has a minimum and maximum value respectively at α=180º and α=90º when β is 90º. It has a minimum and maximum value respectively at α=45º and α=135º when β is 135º. Comparing the results of the twenty experiments saved on the diagram of Fig. 5(c), the maximum value of the static friction coefficients, i.e. 0.266176, occurs under the situation of β=90º and α=90º, and its minimum value, i.e. 0.161847, occurs under the situation of β=90º and α=180º. Maximum difference between the obtained static friction coefficients of Fig. 5(c) is equal to 0.104329. The correction coefficient that is defined as the ratio of maximum to minimum static friction coefficient is equal to 1.644615.

The probable inaccuracy of the experimental data have been attributed to the following sources: (1) Wearing of the steel samples, (2)

Spool eccentricity, (3) Unknown pressure distribution during sanding, (4) Vibration induced by fluid reservoir during the experiment, (5) Inaccuracy in measurement of the weight of water within reservoir, (6) Uncertainty about geometric parameters of the generated surface asperity such as grooves depth and their state of being parallel, and (7) The fact that friction in bearings and between string and spool is not in reality zero, but in this research it has been assumed to be negligible.

Each color in Figs. 5(a, b & c) shows the static friction coefficient between two cylindrical steel samples having sizes equal to those of this article, i.e. f. Each of them has been obtained for a fixed average surface roughness, i.e. R_a, a fixed base angle, i.e. β and a discretely-variable counter body angle, i.e. α.

The latter angle has been considered as 0º, 45º, 90º, 135º and 180º. The average of these five static friction coefficients, namely f_α has been proposed in Table 3.

(a) Average surface roughness: R_a=0.2 micron

(b) Average surface roughness: R_a=0.3 micron

(c) Average surface roughness: R_a=1.1 micron

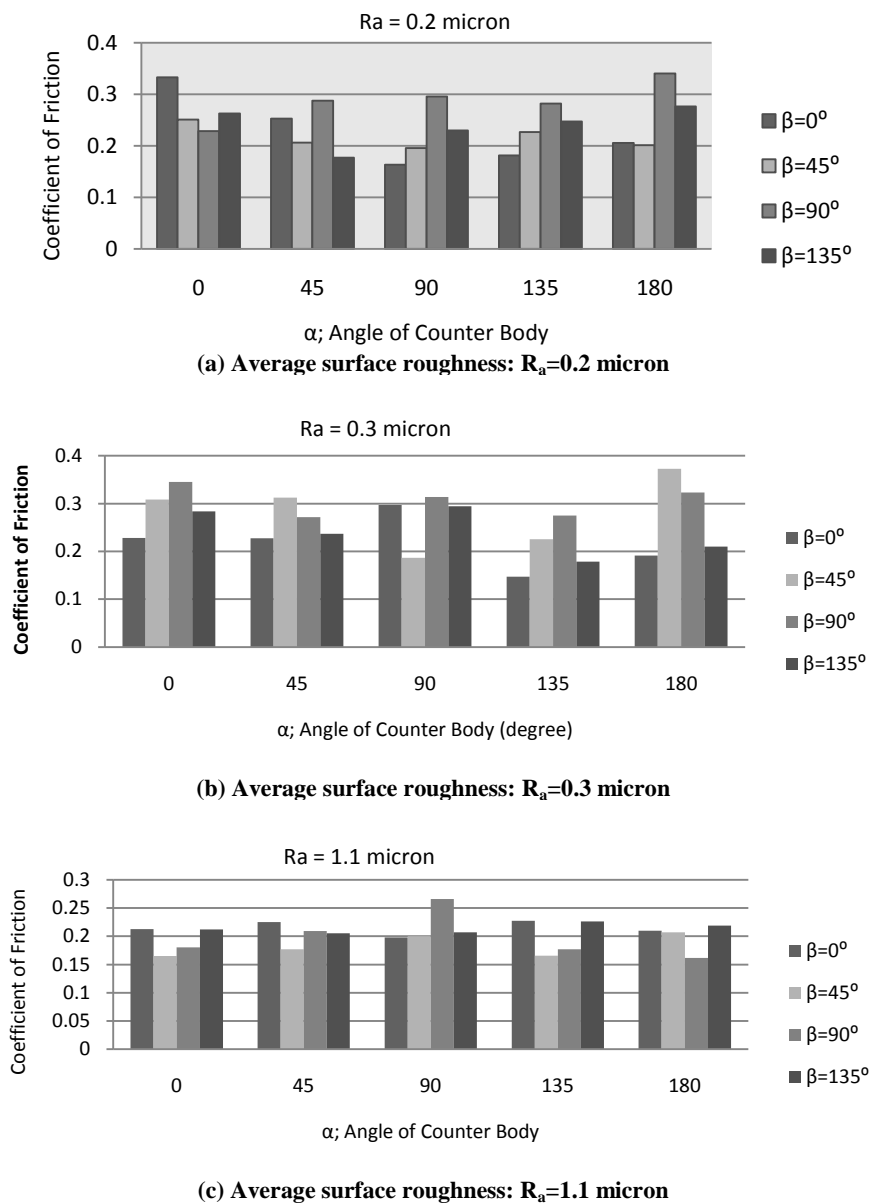Fig. 5. Static friction coefficient between steel samples versus α.

In each of the Figs. 5(a, b & c) four values of β, i.e. 0º, 45º, 90º and 135º have been taken into consideration. Eventually, it is appropriate that Table 3 proposes the average static friction coefficient, namely $f_{\alpha\beta}$ among the mentioned four f_{α}s, for every R_a. Three values, i.e. 0.3, 0.2 and 1.1 μm, have been considered for the average surface roughness of the samples. Table 3 shows that the angle of base; β, is held fixed and the angle of counter body; α, varies.

Table 4 shows the above obtained static friction coefficients in another arrangement.

For each R_a and α, the static friction coefficient has been proposed in terms of the discretely-variable base angle β. Four values have been considered for the base angle as 0º, 45º, 90º and 135º. The average of these four static friction coefficients, namely f_{β} has been proposed in Table 4. In each of the Figs. 5(a, b & c), the five values of 0º, 45º, 90º, 135º and 180º have been considered for α. For each R_a Table 4 proposes the average static friction coefficient, namely $f_{\beta\alpha}$, among the mentioned five f_{β}s. Table 4 shows that the angle of counter body; α, is held fixed and the angle of base; β, varies.

Table 3. Average static friction coefficient; f_{α}s and $f_{\alpha\beta}$ α= 0º, 45º, 90º, 135º or 180º.

R_a (μm)	B (Degrees)	f_{α}	$f_{\alpha\beta}$
0.2	0	0.227164	0.242209
	45	0.216098	
	90	0.286903	
	135	0.238672	
0.3	0	0.218165	0.261376
	45	0.281055	
	90	0.305625	
	135	0.240659	
1.1	0	0.214609	0.202559
	45	0.182909	
	90	0.198878	
	135	0.213841	

Table 4. Average static friction coefficient; f_{β}s and $f_{\beta\alpha}$ β= 0º, 45º, 90º or 135º.

R_a (μm)	A (Degrees)	f_{β}	$f_{\beta\alpha}$
0.2	0	0.26878	0.242209
	45	0.23103	
	90	0.22115	
	135	0.23434	
	180	0.25575	
0.3	0	0.2913	0.261376
	45	0.26191	
	90	0.27276	
	135	0.20669	
	180	0.27422	
1.1	0	0.1925	0.202559
	45	0.20424	
	90	0.21784	
	135	0.19897	
	180	0.19925	

Conclusions

Dry static friction coefficient between two similar steel samples depends on the magnitude and direction of their surface asperities. Its quantitative values have been measured in this article. The numerical results show that the dependency of the friction coefficient upon the magnitude of surface roughness, base or counter body angles representing the asperity directions is very complicated and cannot be analytically predicted. Therefore a table of friction coefficients originated from experiment is more appropriate for the estimation of realistic dry static friction coefficient between two similar steel samples.

Nomenclature

α Angle of counter body measured from stand index

β Angle of base body measured from stand index

AGD Asperity grooves direction

BBA Base body axis

BBI Base body index

CBA Counter body axis

CBI Counter body index

e Arm of the linearly increasing pulling load

F Friction force

f Static friction coefficient; it is a function of α and β

f_α Average of fs; it is not the function of α

f_β Average of fs; it is not the function of β

$f_{\alpha\beta}$ Average of f_αs; it is not the function of α and β

$f_{\beta\alpha}$ Average of f_βs; it is not the function of β and α

g Gravity acceleration

M Moment of the pulling load

M_C Mass of counter body

M_{Cl} Mass of clamp

M_B Mass of base body

M_W Mass of water

M_R Mass of reservoir

N Normal contact force

n Normal support force

R_a Average surface roughness

STD Slide tendency direction

T Linearly increasing pulling load; string tension

References

[1] Kragelsky, I. V., Friction, Wear and Lubrication, in: Tribology Handbook, Vol. 1, VV Alisin-Mir Publishers, Moscow, 1982.

[2] Blau, P.J., Friction, Lubrication, and Wear Technology, in: ASM Handbook, Vol. 18, ASM International, Materials Park, Ohio, 1992.

[3] Menezes, P.L., Kishore and Kailas S.V., Influence of surface texture on coefficient of friction and transfer layer formation during sliding of pure magnesium pin 080 M40 steel plate, J. Tribology, 261 (2006), 578-591.

[4] Sherrington, I., Hayhurst, P., Simultaneous observation of the evolution of debris density and friction coefficient in dry sliding steel contacts, J. Wear, 249 (2001), 182-187.

[5] Hatamleh, O., Smith, J., Cohen, D. and Bradley, R., Surface roughness and friction coefficient in peened friction stir welded 2195 aluminum alloy, J. Applied Surface Science, 255 (2009), 7414-7426.

[6] Sedlacek, M., Podgornik, B. and Vizintin, J., Influence of surface preparation on roughness parameters, friction and wear, J. Wear, 266 (2008), 482-487.

[7] Podgursky, V., Adoberg, E., Surzenkov, A., Kimmari, E., Viljus, M., Mikli, V., Hartelt, M., Wasche, R., Sima, M. and Kulu, P., Dependence of the friction coefficient on roughness parameters during early stage fretting of (Al,Ti)N coated surfaces, J. Wear, 271 (2011), 853-858.

[8] Spijker, P., Anciaux, G. and Molinari, J. F., Relations between roughness, temperature and dry sliding friction at the atomic scale, J. Tribology international, 59 (2012), 222-229.

[9] Sedlacek, M., Podgornik, B. and Vizintin, J., Correlation between standard roughness parameters skewness and kurtosis and tribological behaviour of contact surfaces, J.

Tribology international, 48 (2012), 102-112.

[10] Menezes, P. L., Kishore and Kailas, S. V., Influence of surface texture and roughness parameters on friction and transfer layer formation during sliding of aluminum pin on steel plate, J. Wear, 267 (2009), 1534-1549.

[11] Jackson, R. L., Duvvuru, R. S., Meghani, H. and Mahajan, M., An analysis of elasto-plastic sliding spherical asperity interaction, J. Wear, 262 (2007), 210-219.

[12] François Robbe-Valloire, Statistical analysis of asperities on a rough surface", J. Wear, 249 (2001), 401-408.

[13] Javadi, M. and Tajdari, M., Experimental investigation of the friction coefficient between aluminum and steel, J. Materials Science, 24 (2006), 305-310.

[14] Menezes, P. L., Kishore and Kailas, S. V., Effect of surface roughness parameters and surface texture on friction and transfer layer formation in tin-steel tribo-system, J. of Materials Processing Technology, 208 (2008), 372-382.

[15] Menezes, P. L., Kishore, Kailas S. V. and Lovell, M. R., The role of surface texture on friction and transfer layer formation during repeated sliding of Al-4Mg against steel, J. Wear, 271 (2011) 1785-1793.

[16] Menezes, P. L., Kishore, and Kailas, S. V., Studies on friction and formation of transfer layer when Al-4Mg alloy pins slid at various numbers of cycles on steel plates of different surface texture, J. Wear, 267 (2009), 525-534.

[17] Bhushan, B. and Nosonovsky, M., Scale effects in dry and wet friction, wear and interface temperature, J. Nanotechnology, v 15, n 7, (2004), 749-761.

[18] Menezes, P. L., Kishore, Kailas, S. V. and Lovell, M. R., Friction and transfer layer formation in polymer-steel tribo-system: Role of surface texture and roughness parameters, J. Wear, v 271, issues 9-10, (2011), 2213-2221.

[19] Sadowski, P. and Stupkiewicz, S., Combined effect of friction and macroscopic deformation on asperity flattening, J. Tribology International, 43 (2010), 1735-1741.

[20] Yeo, C. D., Katta, R. R., Lee, J. and Polycarpou, A. A., Effect of asperity interactions on rough surface elastic contact behavior: Hard film on soft substrate, J. Tribology International, 43 (2010), 1438-1448.

[21] Beheshti, A. and Khonsari, M. M., Asperity micro-contact models as applied to the deformation of rough line contact, J. Tribology International, 52 (2012), 61-74.

[22] Mulvihill, D. M., Kartal, M. E., Nowell, D. and HILLS, D. A., An elastic-plastic asperity interaction model for sliding friction, J. Tribology International, v 44, n 12, (2011), 1679-1694.

[23] Javadi, M. and Tajdari, M., A new experimental procedure of evaluating the friction coefficient in elastic and plastic regions, J. Materials Processing Technology, v 177, issues 1-3, (2006), 247-250.

[24] Menezes, P. L., Kishore and Kailas, S. V., On the effect of surface texture on friction and transfer layer formation-A study using Al and steel pair, Wear, 265 (2008) 1655-1669.

[25] Bhushan, B., Contact mechanics of rough surfaces in tribology: multiple asperity contact, Tribology Letters, 4 (1998), 1-35.

[26] Grote, K. H. and Antonsson, E. K., Tribology, in: Springer Handbook of Mechanical Engineering, Sturtz GmbH, Wurzburg, Part B, chapter 5, 2009.